Multi- and Hyperspectral Mineral Exploration of Northwest Queensland, Australia

Directed Problems in Remote Sensing

Matthew Manni

Semester 2, 2012

Table of Contents

List of Figures

List of Tables

Abstract

In this paper, multispectral and hyperspectral remote sensing techniques are used to explore minerals near Mount Isa in North West Queensland, Australia. The area is located adjacent to a mining town that is known for its lead, zinc, silver and copper ore production. Multispectral techniques such as false-colour and band ratio composites were used in conjunction with a principal component analysis (PCA) to locate iron-oxides, sulphates and hydroxyl-bearing minerals. Several composite images revealed that a majority of the northeast section of the study area contains iron-oxides and sulphate minerals, while the northwest portion contains hydroxyl-bearing minerals. Hyperspectral methods were separately applied to both the VNIR and SWIR in order to find more detailed location and abundance maps of particular minerals. The spectral angle mapping (SAM) technique produced classification maps of alunite, hematite, gypsum, galena and tincalconite. The linear spectral unmixing technique was also used to create abundance maps of these same minerals. These methods resulted in much more detailed mineral identification maps which mostly agreed with the multispectral results. Both the multispectral and hyperspectral analyses displayed that there are potential mining opportunities in the northern region of the study area. Although, field surveys need to be conducted in order to confirm the results and continue the mineral exploration process.

1. Introduction

Remote sensing is the science of using sensors to detect and classify objects on Earth's surface by obtaining information on the interaction of electromagnetic radiation with the surface via aircraft or satellite. This concept has been used for many years and with various applications including land use, agriculture, climate change, natural hazards and geology. Another highly useful application is mineral exploration, due to its implications on Earth's resources. There will always be demand for mineral extraction and locating ore deposits in order to sustain continuous development. Geologists and spatial analysts can use multispectral and hyperspectral remote sensing images to identify, locate and map mineral deposits on regional scales. This includes observing the lithology, structure and other topographic features to detect minerals.

Multispectral and hyperspectral images are also often used for target detection, material identification and mapping, and mapping details of surface properties. Imagery, digital image processing, spectral analysis, remote mapping and field work can all be used together with the help of GIS to locate ore deposits and minerals. The images are processed and analysed for several purposes including land cover analysis, geological exploration, lithological classification and mapping, change detection, surface deformation and erosional patterns (Goetz & Rowan, 1981). All of these applications are used to help monitor environmental changes and detect natural resources (Figure 1). Due to the increase in population and high demand for resources, there is even more of a need for remotely sensed mineral exploration in search of more subtle deposits at remote locations.

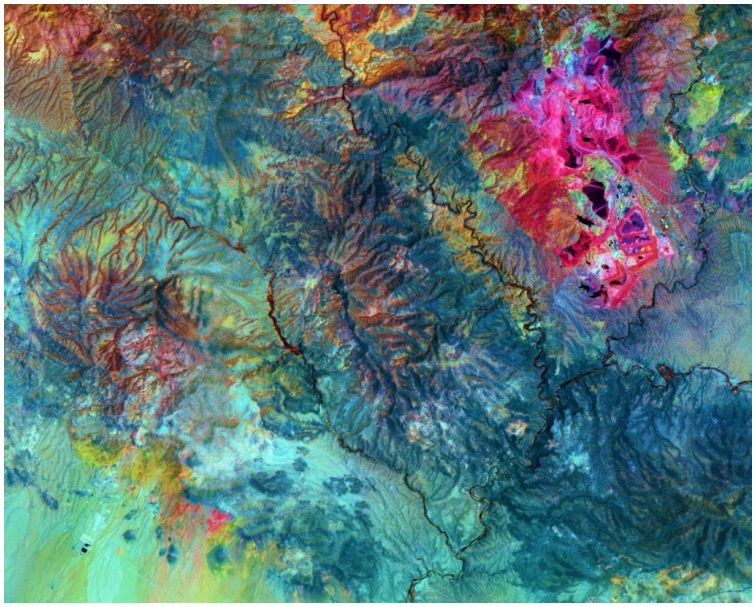

Figure 1: Example of Multispectral Image for Mineral Exploration [Source: Oliver and van der Wielen (2006)]

Remote sensing can be used to measure many aspects of mineral exploration. Aerial photos, from both aircraft and satellite, are used to identify topographic surface features that imply the subsurface geology. Some of these features include differential erosion, outcropping rock formations, drainage patterns, folds, faults, fractures and contacts (Rajesh, 2004). These features can be compared with other potential target areas in a region in order to find minerals. Some of the most useful features that can be observed directly from an aerial photo are faults, fractures and contacts which provide a depositional environment for hydrothermal or magmatic fluids in areas of known mineralisation (Tukiainen and Thomassen, 2010).

By mapping the geology of the area and searching for recognisable structural trends, the data can be used to localise ore deposits. Geologists can also apply imagery to geological surveys, alteration zone mapping and geomorphology surveys to indicate variations in mineralogical compositions. Collecting data such as alteration products of mineral deposits and changes in plant cover are helpful in identifying changes in lithology. These images can be used to interpret the actual surface lithology of the land in order to identify clays, soils and rock composition. In many cases, satellite imagery from multispectral or hyperspectral sensors are used to produce the spectral signature of specific rock materials or minerals, which can be used to recognise hydrothermally altered rocks and find similar objects in images of the area.

In this study, multispectral and hyperspectral images were used to identify minerals in an area near Mount Isa in Northwest Queensland Australia. Multispectral techniques such as band ratioing, false-colour composites and principal component analysis (PCA) are used to identify certain types of minerals in the area, such as iron oxides and hydroxyl-bearing minerals. A more complicated process is used for identifying minerals in hyperspectral images. Spectral unmixing and subpixel methods were used to locate and determine the abundance of various materials based on spectra measurements from NASA's Jet Propulsion Laboratory (JPL). The data used in this study include multispectral images from the Landsat 5 Thematic Mapper (TM) and hyperspectral images from Hyperion (Table 1). The USGS, United States Geological Survey, has provided these images free of charge. The images were both taken in an area adjacent to Mount Isa in October, 2003.

Table 1: Description of Image Specifications

Satellite	Path/Row	Central Latitude	Central Longitude	Cloud Cover	Quality & Look Angle	Date
Landsat 5 TM	99/74	-20.227	139.543	0%	Quality: 9*	30/09/03
Hyperion	99/74	-19.841	139.626	0%	-0.0929°	06/09/03

*Excellent quality with no issues or errors

2. Geology of the Study Area

The study area is located within the Selwyn Range in Northwest Queensland, Australia near a small mining town in Mount Isa (Figure 2). This area is commonly known for their lead (Pb), zinc (Zn), silver (Ag) and copper (Cu) ores, with several mines already in operation. There are two different ore bodies that have been extensively faulted in this area: a lower lead-zinc-silver ore and an upper copper ore (Conaghan et al., 2003). These ore bodies are interbedded within volcanic material and can reach up to 50 metres in thickness (McDonald et al., 1997). Since their discovery in the 1920s, the Mount Isa Mines have produced over 6 million tonnes of copper ore with 3.3% Cu and around 5 million tonnes of silver-lead zinc ore with 154 g/t Ag, 5.4% Pb and 6.5% Zn (Conaghan et al., 2003). The Pb-Zn-Ag ore bodies have been known to contain the following minerals: galena, sphalerite, pyrite, pyrrhotite and freibergite; while the Cu ore bodies are known to contain chalcopyrite, pyrite and pyrrhotite (Conaghan et al., 2003).

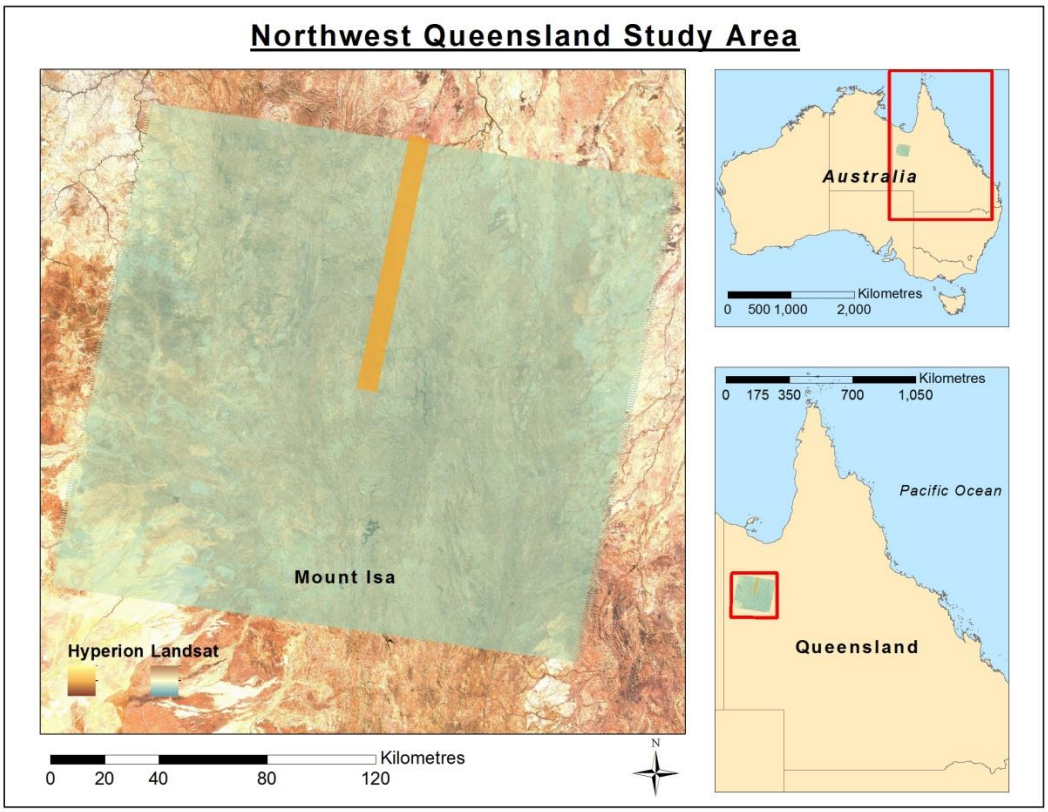

Figure 2: Location Map of Study Area

The rocks in this study area are contained within the Mount Isa Orogen, which is over 50,000 km^2 at about 1865 Ma old, and can be divided into three provinces: the Western Fold Belt Province, the Kalkadoon-Ewen Province and the Eastern Fold Belt Province (Figure 3, McDonald et al., 1997). The Mount Isa Orogen has a complex history of deformation which has experienced several different periods of extension, shortening and strike-slip faulting (McDonald et al., 1997).

The minerals have formed from millions of years of this deformation which has created steeply west-dipping bedding. Most of the ore bodies are contained within the Urquhart Shale Formation, a 5-km-thick metamorphosed sequence of Proterozoic carbonate siltstones, mudstones and shales (Conaghan et al., 2003). In some areas, the Pb-Zn-Ag ore bodies are interbedded with lobes of silica-dolomite from the older Eastern Creek Volcanic Formation and lie beneath the Cu ore bodies contained within the Urquhart Shale formation (McDonald et al., 1997).

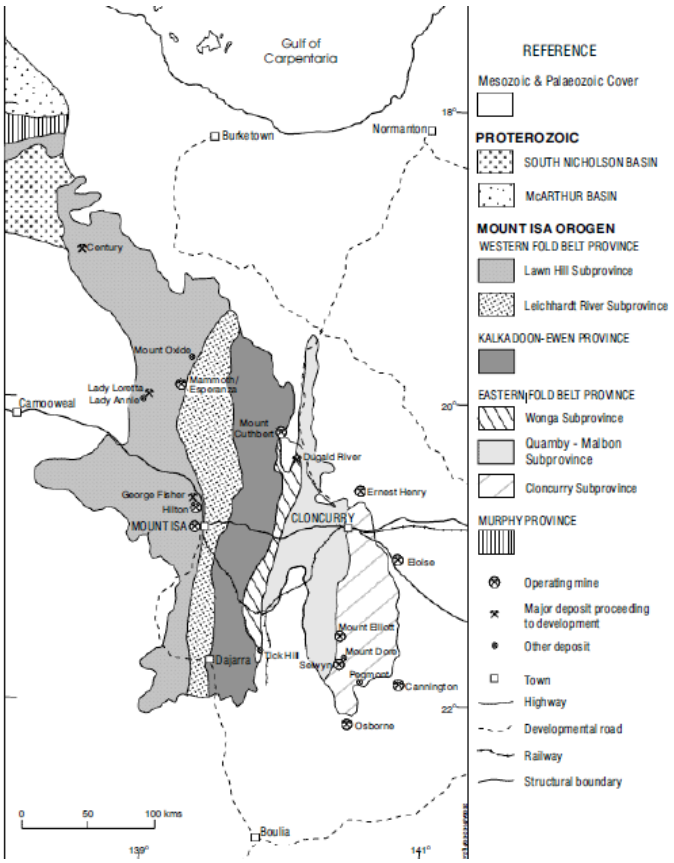

Figure 3: Geological Map of Mount Isa [Source: McDonald et al. (1997)]

3. Sensors and Background Theory

A variety of remote sensing tools can be used together to analyse images and assist in mineral exploration. Before the images are analysed and used to their full extent, the image data must be processed to enhance the image in order to identify minerals and ore deposits. The analysis and interpretation of image data are mostly based on the use of spectral libraries. This allows for locating target areas with hydrothermal mineral alteration by discriminating individual mineral species and alterations specific to a particular type of mineral from a spectral library (Amax, et al., 1983).

The minerals are identified by their absorption characteristics at certain wavelengths as seen in their spectral signatures (Figure 4). The reflective spectra of most common minerals are often found between 0.4 and 2.5 micrometres (µm) (Rockwell, 2004). Absorption features of hydrothermally alteration minerals found in the shortwave infrared (SWIR) spectrum are often used to identify carbonate materials and hydroxyl-bearing minerals (clays), with absorption features at 1.65 µm, 2.2 µm, and 2.3 µm (Rajesh, 2004). The visible near infrared (VNIR) is usually used to identify iron-bearing minerals and hydroxides, with absorption features at 0.35 to 1.5 µm (Rajesh, 2004).

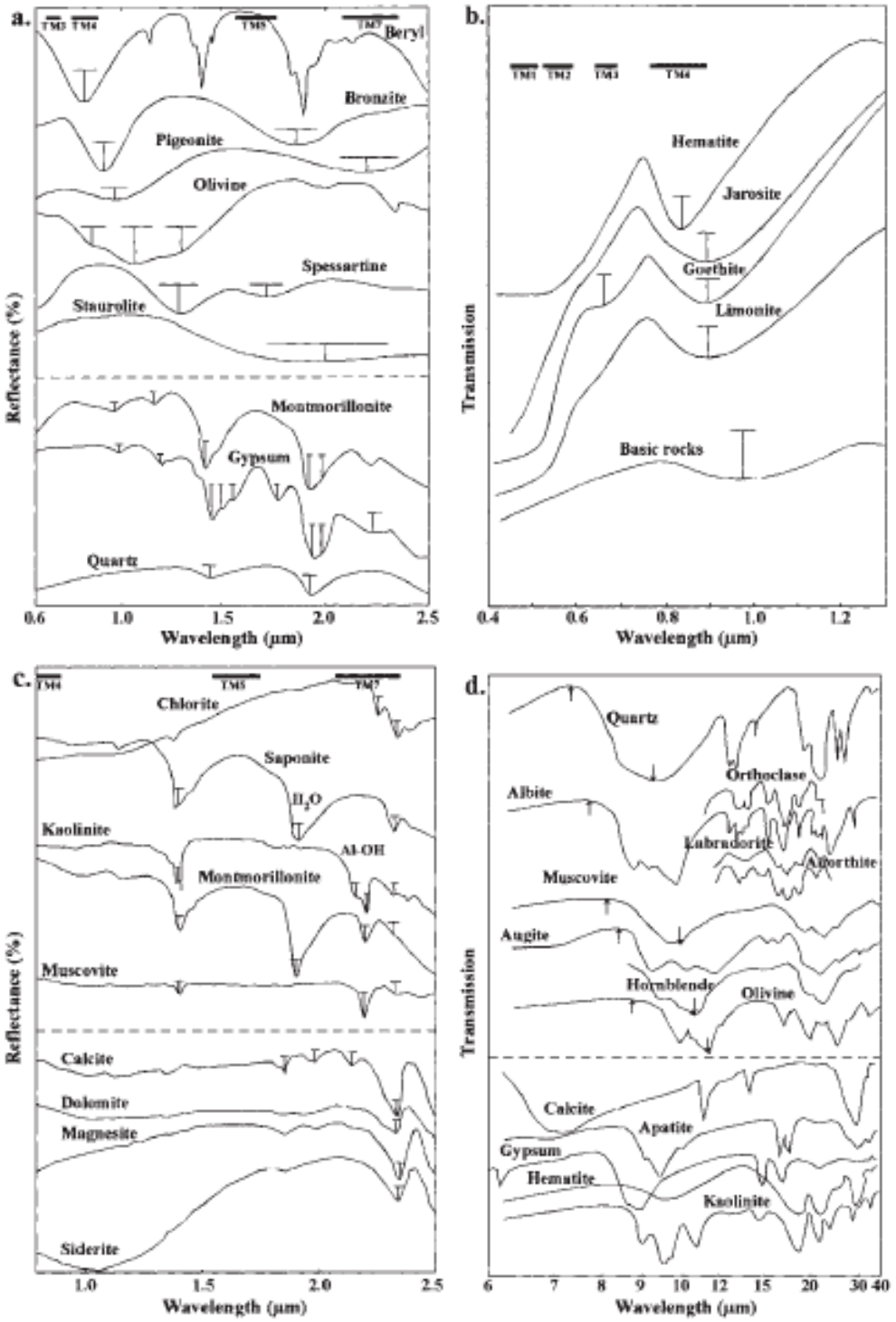

Figure 4: Spectra of Common Minerals: a) iron-bearing minerals (above dashed line) and minerals containing water (below dashed line), b) iron oxides and hydroxides, c) clay minerals (above dashed line) and carbonate minerals (below dashed line), d) selected silicates (above dashed line) and non-silicates (below dashed line). Absorption features are shown by T-shaped symbols. [Source: Rajesh (2004)]

3.1 Landsat 5 Thematic Mapper

The Landsat 5 satellite was first launched by NASA in 1984 with both the Multispectral Scanner (MSS) and the Thematic Mapper (TM) sensors attached; however collection of MSS data was terminated in 1992. This sun-synchronous satellite orbits at an altitude of 705 km and provides a 16-day, near-polar orbit cycle

that can capture 170 km x 185 km (swath width) scenes of Earth's surface (Mshiu, 2011). The output images are projected with the WGS84 – UTM map projection and most images are L1T radiometrically and terrain corrected with a digital elevation model (DEM). Landsat TM images consist of seven spectral bands with a spatial resolution of 30 m for Bands 1-5 and Band 7, and a spatial resolution of 120 m for thermal infrared Band 6 (Table 2, Harris et al., 1998).

Table 2: Landsat TM Specifications

	Landsat 5	Wavelength (micrometres)	Resolution (metres)
Thematic Mapper (TM)	Band 1	0.45-0.52	30
	Band 2	0.52-0.60	30
	Band 3	0.63-0.69	30
	Band 4	0.76-0.90	30
	Band 5	1.55-1.75	30
	Band 6	10.40-12.50	120* (30)
	Band 7	2.08-2.35	30

*Resampled to 30-m pixels

3.2 Multispectral Techniques

The methods used to locate minerals within a multispectral scene are fairly standard for any mineral exploration study with that type of imagery. Multispectral techniques such as band ratio combinations and principal component analysis (PCA) are used to identify certain types of minerals in the area, such as iron oxides and hydroxyl-bearing minerals. Mineral identification maps can then be produced using simple band ratios and false colour composites that correspond to absorption features for a particular mineral.

The basic steps for image processing and analysis of multispectral images include (Sabins, 1999):

a) Image restoration by calibrating and atmospherically correcting the image;
b) Image enhancement by contrast stretching;
c) Information extraction by band ratioing and PCA

Calibration and correction are used to filter out random noise and correct for geometric distortions and atmospheric scattering. Several methods such as contrast enhancement, density slicing and edge enhancements can be used to improve the image for a clearer display of the scene (Sabins, 1999). Lastly, to extract information for analysis, the pixels in the image can be classified after ratioing certain bands or applying a principal component analysis.

Band ratios are extremely useful for evaluating the spectral properties of Earth by revealing the reflectance differences between certain bands (Harris et al., 1998). Band ratio 5/7 is used to identify the presence of hydroxyl-bearing (clays) or carbonate materials, a ratio of 3/1 can be used to identify iron-oxides and sulphates, and a ratio of 5/4 can identify ferrous materials (van der Meer et al., 2012). High ratios indicate hydrothermally altered rocks, while low ratios indicate unaltered rocks. False-colour composites can be created with these band ratios to produce mineral identification maps. A false-colour composite of R = 5/7, G = 3/1, and B = 5 can produce a normalised image for mineral identification or a

ratio image of R = 3/5, G = 3/1, and B = 5/7 can also be created to identify iron-bearing and clay materials (Harris et al., 1998).

The principal component analysis (PCA) is a linear transformation that converts correlated dimensions to uncorrelated dimensions, thus reducing data dimensionality by condensing spectral information into separate principal components to enhance features (Goetz et al., 1985). This is applied to the images to extract specific spectral responses and identify hydrothermal alteration. The PCA is basically a statistical technique used to target minerals based on enhancing the spectral reflectance features of geological materials by suppressing irradiance effects that dominate bands (Crosta et al., 2003). To complete the analysis, the feature-oriented principal component selection (FPCS) method is used to select principal components by their unique absorption features of minerals based on the eigenvector matrix of the multispectral image (Goetz et al., 1985). This allows for an analysis of the spectral signatures of FPCS images which compares the extracted image spectra with the library spectra. The final product is a more detailed mineral identification map compared to that of band ratioing.

3.3 Hyperion

On-board the satellite Earth Observing 1 (EO-1), launched in 2000 by NASA, there is a high resolution hyperspectral sensor called Hyperion. It is used mostly for mineral mapping in conjunction with multispectral images, such as ASTER image data. This sun-synchronous satellite is very similar to Landsat, orbiting at an altitude of 705 km and providing a 16-day, near-polar orbit cycle. The sensor can capture a 7.75 km (swath width) x 100 km scene over Earth's surface, collecting 220 unique spectral channels ranging from 0.357 to 2.576 µm with a bandwidth of 0.01 µm (Wand & Zheng, 2010). Hyperion data yields 242 spectral bands, with bands 1-70 for VNIR spectral range and bands 71-242 for SWIR spectral range. From the 242 bands contained within Hyperion data only 198 bands are calibrated due to the detector's low responsivity and only 196 bands are unique due to an overlap between the VNIR and SWIR (Dehnavi et al., 2010). The instrument operates in pushbroom mode, with a spatial resolution of 30 m for all bands and 16-bit radiometric resolution. Hyperion has a relatively low signal-to-noise ratio (SNR) of about 40-190, depending on wavelength (Bishop et al., 2011). The output images are also projected with the WGS84 – UTM map projection and most images are L1Gst terrain and radiometrically corrected.

3.4 Hyperspectral Techniques

Hyperspectral data can help identify regions of mineral resources by using distinct absorption features of minerals and comparing them to field or laboratory references. A more complex process is needed for mineral exploration with hyperspectral images. Two types of methods can be used to analyse the image and map mineral abundances: spectrum matching and subpixel methods.

The basic steps for image processing and analysis of hyperspectral images include (Bishop et al., 2011):

a) Image calibration and atmospherically correcting the image;
b) Transform reflectance data to minimise noise and find data dimensionality;
c) Locate purest pixels;
d) Identify endmember spectra based on spectral library;
e) Map abundance estimates of endmembers

Before applying the two mapping methods mentioned above, the data volume needs to be reduced by applying the maximum noise fraction (MNF) transform, which minimises noise in the data and determines the data dimensionality (Denniss et al., 1996). This reduces the computational requirements for the following processes. Once the data dimensionality is determined, the pixel purity index (PPI) is used to identify the spectrally pure, or extreme, pixels in the hyperspectral data (Denniss et al., 1996). These pixels

are then examined using an n-dimensional visualizer which uses a scattergram tool to identify endmembers by locating and clustering the purest pixels in the n-dimensional space (van der Meer et al., 2012). This finds clusters of spectrally purest pixels, of different mineralogies, which can be used to create a spectral library of endmember spectra based on the purest pixels. The endmember library can then be used in the abundance mapping methods described below (Denniss et al., 1996).

Spectrum matching methods compare the spectral similarity of referenced spectra from the field or laboratory with image spectra (van der Meer et al., 2012). In order to discriminate and map mineral species, spectrum matching methods such as the spectral angle mapper (SAM) or mixture tuned matched filtering (MTMF) techniques can be applied to hyperspectral images. The SAM method matches image spectra to reference spectra in n-dimensions by comparing the angle between the endmember spectrum and each pixel vector in the n-dimensional space (van der Meer et al., 2012). MTMF is a mapping method based on matched filtering and linear spectral unmixing which finds the abundances of the endmembers by maximising the response of the known endmembers and minimising the response of unknown background (Bishop et al., 2011).

Subpixel methods quantify the relative abundance of materials within a pixel by unmixing hyperspectral images (van der Meer et al., 2012). The most common subpixel method is linear spectral unmixing, as opposed to a non-linear method. This technique takes the pixel spectra and the endmember spectra to solve for the abundance of each endmember within each pixel. The linear spectral unmixing method finds the abundances of materials within each pixel by assuming that the pixel reflectance in each band is equal to a linear combination of the endmember spectra within the pixel (Bishop et al., 2011).

4. Methods

In this study, the spectral analysis of multispectral and hyperspectral data was conducted using the ENVI software application developed by Exelis Visual Information Solutions (Rockwell, 2004). All data was provided by the USGS and was analysed using common mineral exploration analysis methods to locate and identify minerals within the scene, as described in Section 3.

4.1 Multispectral Methods

The Landsat 5 TM data was originally loaded into ENVI using the MTL file that was provided in the download from the USGS Global Visualisation Viewer website. The original images are L1T products, standard terrain corrected, which are radiometrically and geometrically corrected using pre-processing methods and a DEM for accuracy. Further pre-processing was conducted in order to analyse the data within ENVI. The Landsat calibration tool was first used to convert the digital numbers of each pixel to the spectral radiance. This yields the reflectance of each pixel in units of radiance as watts per square metre per steradian per micrometre ($W/(m^2*sr*\mu m)$). The data was then atmospherically corrected using the Dark Subtract tool within ENVI, removing any atmospheric scattering and noise in the data.

A subset of the Landsat image was used for the rest of the analyses to match the same extent used for the Hyperion image. Contrast stretching was then applied using a linear transform in order to enhance the display of the data within the image. The linear transform sets a minimum and maximum input value to 0 and 255 respectively and all other values in between are linearly aligned to intermediate output values (Mshiu, 2011). Band ratios were then created with the corrected and enhanced data (Table 3). Several other band ratios were produced for supplementing the false-colour composite images.

Table 3: Band Ratios of Landsat TM Data

Band Ratio	Useful for Mapping
5/7	Emphasizes hydroxyl-bearing (clays) minerals and carbonates
3/1	Emphasizes iron oxides and sulphates
5/4	Emphasizes ferrous iron minerals
4/3	Discriminates vegetation
3/5, 4/1, 4/5, 5/1, 3/7, 4/2, 1/2, 1/3	Supplementary to false-colour composite images

False-colour composite images were then produced in order to identify the location of certain types of minerals based on their composition (from Table 3). Several composite maps were created emphasizing the different minerals and hydrothermally altered areas which were used to help locate potential areas in which ore bodies could be present. Band composites of a) 7, 4, 1 (R, G, B) and b) 7, 4, 2 were used to help identify these mineral types. In the resulting images, the yellow, tan or light brown areas identify the presence of iron oxides and sulphates, the teal or light green areas indicate carbonates or clay deposits, the black areas represent water bodies and the green areas identify vegetation (Imbroane et al., 2007).

Band ratio composites of c) 3/1, 5/7, 5/4 (R, G, B), d) 5/7, 3/1, 5 and e) 3/5, 3/1, 5/7 were also used to identify mineral types. Composition c) results in an image with yellow specifying the hydrothermally-altered areas, black representing water bodies, dark green representing vegetation, light green specifying the clay-rich rocks and red, magenta or pink identifying iron oxides and similar mineral rocks (Imbroane et al., 2007). Composition d) and e) show similar results but display different colours that represent the minerals and are more easily distinguishable.

A principal component analysis was then conducted in order to identify areas of hydrothermal alteration, thus locating potential ore bodies. Band set 1-4-5-7 was used for hydroxyl-bearing minerals and carbonates, mapped into principal component 1 (PC1), while band set 1-3-4-5 was used for iron-oxides, mapped into principal component 4 (PC4) (van der Meer et al., 2012). These PCs were selected based on the eigenvector matrix produced by the principal component tool used in ENVI (Table 3 & 4). The PC containing the largest spectral contrast, or eigenvector difference, will minimise the spectral response from other materials in the image (Crosta et al., 2003). This PC will determine the pixels likely to contain certain minerals.

Table 4: Eigenvector Matrix of PCA Bands 1-4-5-7

Eigenvector	PC1	PC2	PC3	PC4
Band 1	0.172284	0.486178	0.675107	0.527428
Band 4	0.369448	0.754194	-0.269060	-0.471494
Band 5	-0.465392	0.368474	-0.581345	0.556485
Band 7	0.785644	-0.243000	-0.365891	0.435704

Table 5: Eigenvector Matrix of PCA Bands 1-3-4-5

Eigenvector	PC1	PC2	PC3	PC4
Band 1	-0.194063	-0.421492	-0.536694	-0.704729
Band 3	-0.322327	-0.286521	-0.573259	0.696696
Band 4	-0.126438	-0.806091	0.572424	0.080998
Band 5	0.917855	-0.300777	-0.235934	0.106818

4.2 Hyperspectral Methods

In order to easily load the Hyperion data into ENVI, the Hyperion tool was downloaded from the Exelis website, which allows for faster importing and hyperspectral calibration. This is needed because of the large volume of data that is produced from hyperspectral sensors. Again, the data was downloaded from the USGS Global Visualisation Viewer website. The original images are L1Gst products, systematic terrain corrected, which are radiometrically corrected and resampled for geometric correction using a DEM for accuracy. After importing and calibrating the images, the data was then atmospherically corrected using the Fast Line-of-sight Atmospheric Analysis of Spectral Hypercubes (FLAASH) tool in ENVI. This tool corrected the image for atmospheric scattering based on various parameters provided within the metadata.

The VNIR and SWIR use two different spectrometers so two spectral analyses were conducted because of the different noise structures produced. Also, not all bands were used in this analysis due to uncalibrated and overlapping bands: VNIR – bands 8-57 and SWIR – bands 79, 83-119, 133-164, 183, 184, 188-220. A maximum noise fraction (MNF) transformation was first applied to the data set in order to reduce the data volume. This process helped reduce the computational requirements while segregating the noise in the image and determining the data dimensionality. The VNIR had a data dimensionality of 12 bands and the SWIR had a data dimensionality of 15 bands based on the eigenvalues from the MNF transform (Figure 5).

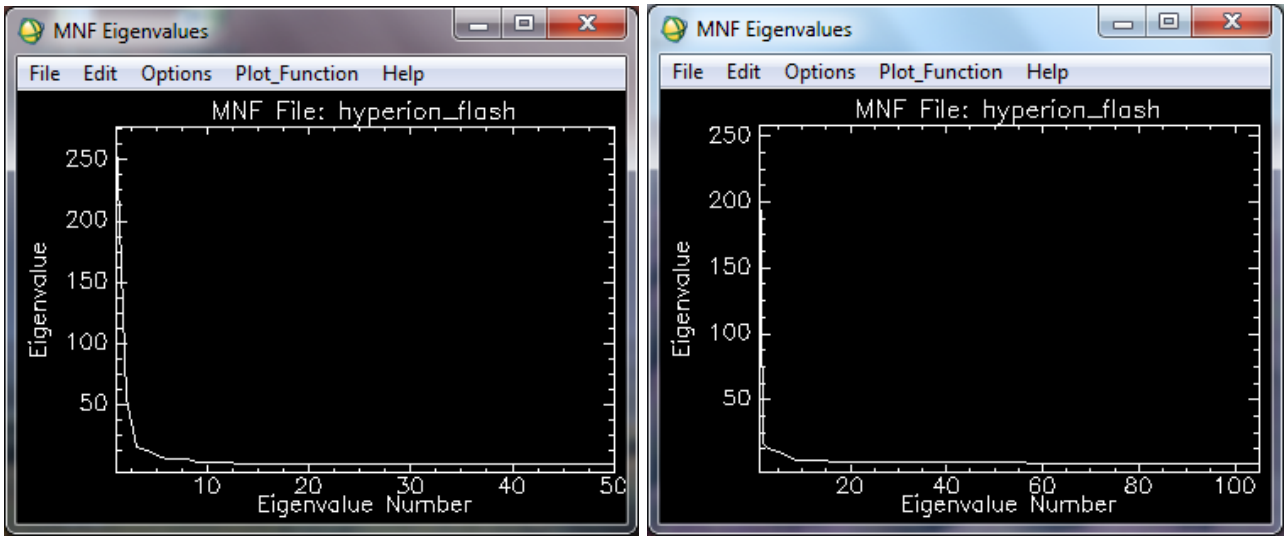

Figure 5: MNF Eigenvalues. Left: VNIR Bands. Right: SWIR Bands.

A pixel purity index was run on the MNF transform results, excluding the noise bands, in order to locate the spectrally purest pixels in the data. With the PPI, a region of interest (ROI) was created to select only the purest pixels from the MNF transform data. The N-dimensional visualizer within ENVI was then used to locate, identify and cluster the purest pixels from the MNF transform and PPI results by rotating a scattergram to select endmembers. For the VNIR, 12 dimensions were used and for the SWIR, 15 dimensions were used in the scattergram. The selected endmembers were grouped into several classes and stored as separate ROIs to be used in the mapping methods (Figure 6). The VNIR produced six classes from the endmembers and the SWIR produced 5 classes. Endmembers where then compared with the JPL spectral library to find matching minerals using the spectral analyst tool in ENVI. The endmembers were relabelled to the most appropriate minerals based on the highest scoring mineral from the spectral library.

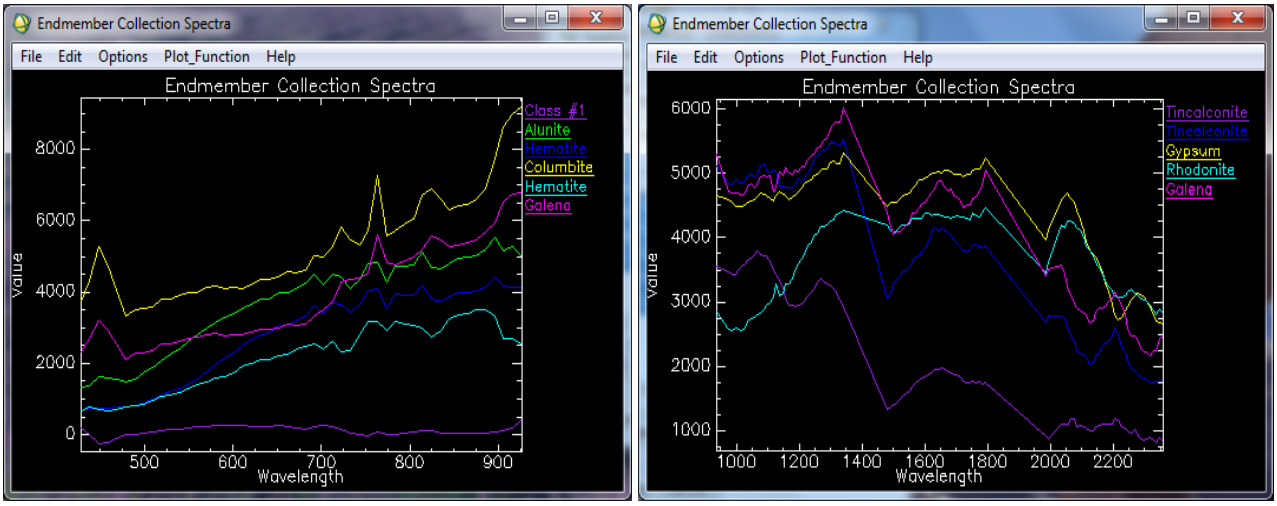

Figure 6: Endmember Sepctra Plots. Left: VNIR Bands. Right: SWIR Bands.

Two of the three mapping methods mentioned before were used in this study to map mineral locations and abundances: spectral angle mapper (SAM) and linear spectral unmixing. ENVI has automated tools that enable the user to input the necessary data in order to apply these methods. The SAM method was used on the FLAASH corrected hyperspectral data to match pixels to reference spectra. The selected endmember spectra, as ROIs, were used in this method to find the matching spectra within the image. This resulted in a classification map of the endmembers within the entire image. The linear spectral unmixing method was used to determine the relative abundances of materials based on the materials spectral characteristics. This method was also applied on the FLAASH corrected data in order to find the abundance of each selected endmember within each pixel. This resulted in a series of gray-scale images, one for each endmember, with higher abundances represented by brighter pixels.

5. Results and Discussion

5.1 Multispectral Results

From the Landsat dataset, it is easy to find general areas of certain mineral types based on the results from false-colour composites and the PCA. The images consisting of band compositions 742 and 741 give very similar results and only help as an initial analysis of locating such minerals as iron-oxides, sulphates, hydroxyl-bearing minerals and carbonates. Within the subset of the original Landsat image (7.75 km x 100 km), there is a distinct contact line separating the iron-oxides and sulphates from the clays and carbonates (Figure 7). The north-east portion of the image is mostly composed of the iron-oxides and sulphates, while the north-west portion of the image is dominated by clays and carbonates. The southern section is a mix of all of those mineral types, which are intertwined with other sedimentary rocks as well. Examining the band ratio composites gives more information on the area.

Figure 7: False-colour Composite (b) 742 of Landsat Image

The band ratio composites of bands 3/1, 5/7, 5/4, bands 5/7, 3/1, 5 and bands 3/5, 3/1, 5/7 were used to display more detailed false-colour composites of the Landsat image (Figure 8). All composites show similar results with a different colour coordination for each one. With these images, iron oxides or sulphates, carbonates or hydroxyl-bearing minerals and hydrothermally altered rocks could be identified. Again there is a distinct contact line separating the types of minerals based on their composition. There are also several lineament features that can easily be identified and used for mapping the geology of the area. For mineral exploration, these images only help provide a more precise location map of the aformentioned mineral types and hydrothermally altered rocks. For the most part, the same pattern is found in which the iron-oxides and sulphates are in the north-east and the carbonates and clays are in the north-west. However, there seems to be more hydrothermally altered rocks in the western half of the image. This indicates that a large extent of the carbonte/clay mineral area has been hydrothermally altered and could therefore be a prime location for potential mining.

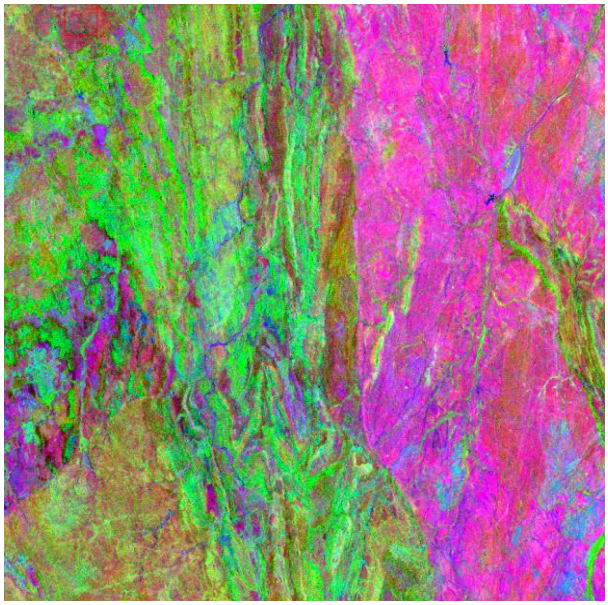

c)

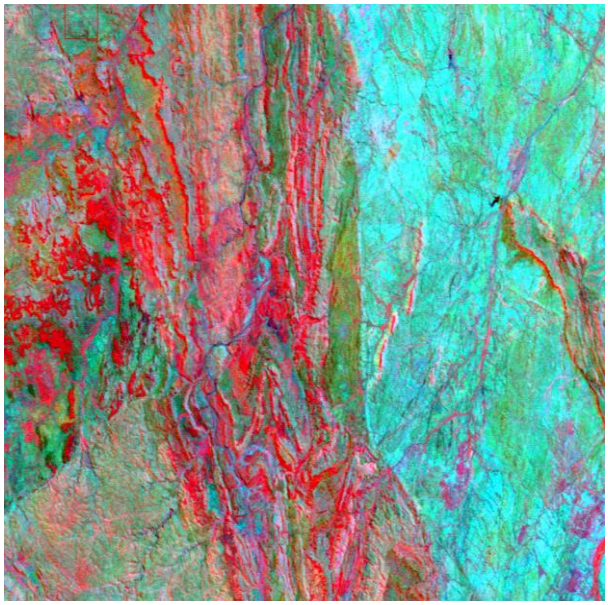

d)

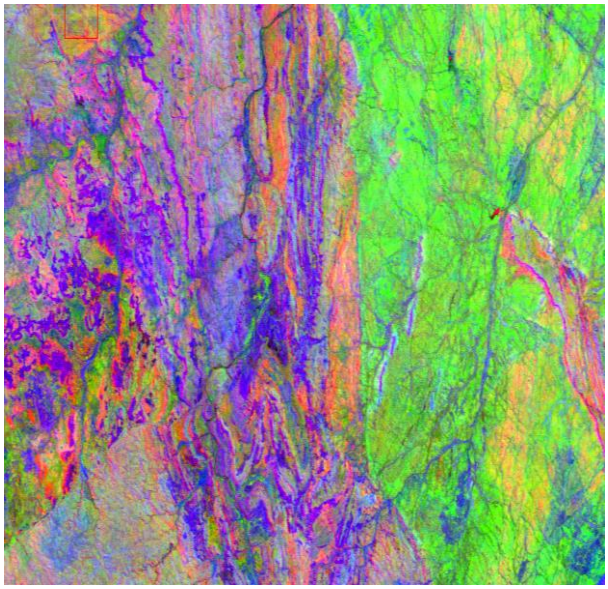

e)

Figure 8: Band Ratio Composites: (c) Bands 3/1, 5/7, 5/4 of Landsat image. Pink areas indicate iron oxides and sulphates, light green areas indicate carbonates and clay minerals and yellow areas indicate hydrothermally altered rocks. (d) Bands 5/7, 3/1, 5 and (e) bands 3/5, 3/1, 5/7 of Landsat image show similar results with a different colour coordination.

The PCA is another tool that was used to help distinguish mineral types from other surface materials. PC Band 1 was used on band set 1-4-5-7 in order to identify clays and carbonates as low, dark, responses (Figure 9). PC Band 4 was used on band set 1-3-4-5 in order to identify iron-oxides and sulphates as low responses also (Figure 10). This analysis resulted in an even more detailed location map of mineral types. The extent of the iron-oxides and sulphates present in these images is very similar to that of the band ratio composite images. However, the extent of the carbonates and clays is much smaller and defined with the PCA. The north-west portion of the image displays much less dark responses than expected, based on the band ratio composites. The clay-rich minerals and carbonates are mostly in mid-west region of the image according to the PCA.

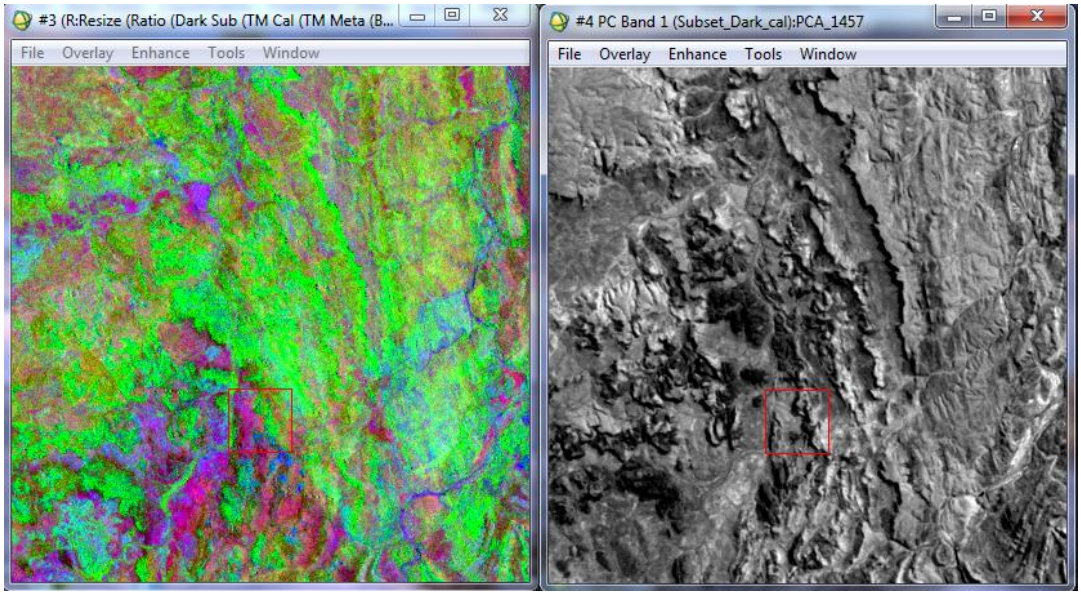

Figure 9: PC Band 1 of Band Set 1-4-5-7

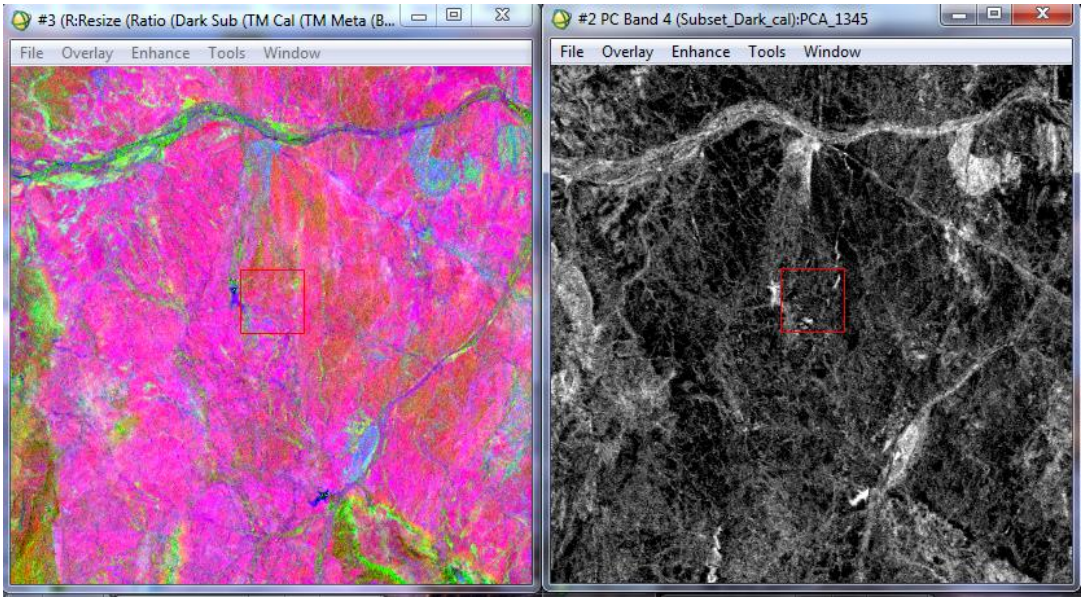

Figure 10: PC Band 4 of Band Set 1-3-4-5

The false-colour composites, band ratio composites and principal component analysis all helped contribute to locating different mineral types within the image. Each analysis should be used in conjunction with another in order to assist with identifying the target areas. The ore bodies commonly found within this area are mostly composed of iron and sulphur-rich minerals, so examining the locations of iron-oxides and sulphates is better for determining potential mines, rather than carbonates or clay-rich minerals. However, examining the areas with hydrothermally altered rocks could be another useful resource for mineral exploration.

5.2 Hyperspectral Results

The hyperspectral data can be easily compared with the multispectral data due to the high number of channels and small bandwidth. A Hyperion image consisting of bands 215, 54, 18 is almost identical to a Landsat TM image consisting of bands 7, 4, 2 (Figure 11). Hyperspectral images have so many more applications for mineral exploration than multispectral images because of the size and detail of the data.

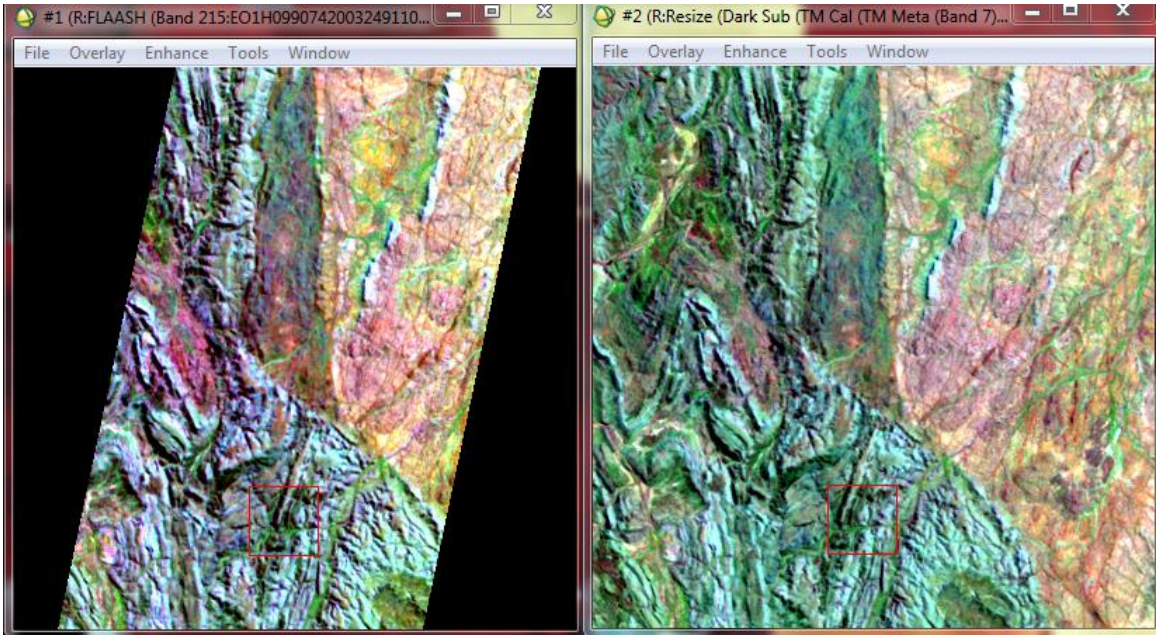

Figure 11: Hyperspectral and Multispectral Comparison.
Left: Hyperion bands 215, 54, 18. Right: Landsat 5 TM bands 7, 4, 2.

5.2.1 VNIR Results

The analysis of the VNIR spectrum helped locate and map several iron-bearing and sulphate minerals in the study area. After analysing the spectral properties of the selected endmembers, the following minerals were found by the spectral analysis of the data: alunite, hematite, columbite and galena. Only one of the selected endmembers could not be identified by the spectral analyst with the JPL library. The SAM method produced a classification map of the four identified minerals, but mostly mapped alunite and hematite. The blue-coloured areas on the map represent hematite (Fe_2O_3), an iron-oxide mineral, and the green-coloured areas represent alunite ($KAl_3(SO_4)_2(OH)_6$), a hydroxyl-bearing sulphate mineral. This method compares quite well with the multispectral analysis of the area (Figure 12).

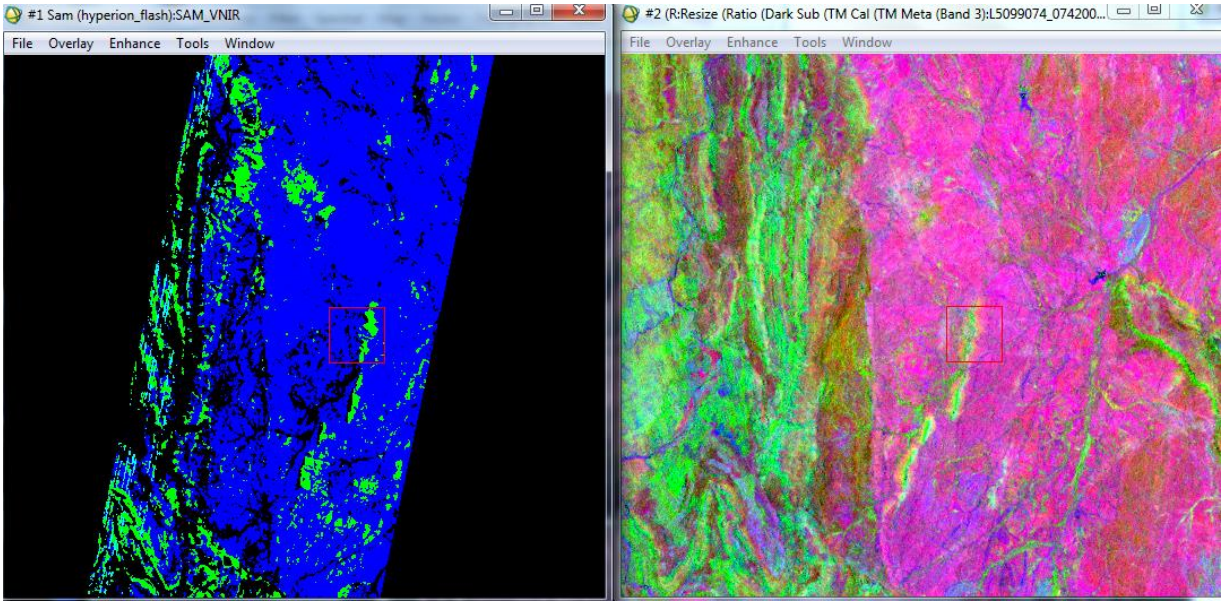

Figure 12: VNIR SAM Classification Map.
Left: SAM Classification. Right: Landsat 5 TM band ratio 3/1, 5/7, 5/4.

The linear spectral unmixing method produced several gray-scale images of each mineral showing the bright pixels as high abundances of that mineral within the image. This was mostly useful for the alunite and hematite, the most classified endmembers from the SAM method (Figure 13 and 14). However it also produced a useful abundance map of galena (PbS), a sulphide mineral common in lead ore, which was not mapped (black) in the SAM method (Figure 15). Mapping the abundances of these classes with the spectral unmixing method produced much more detailed maps than the SAM classification method, which produced a very broad classification map. Again, this method shows similar results to the multispectral analyses in which the location of the mineral types are the same, however the spectral unmixing technique goes further and maps the abundance of each mineral.

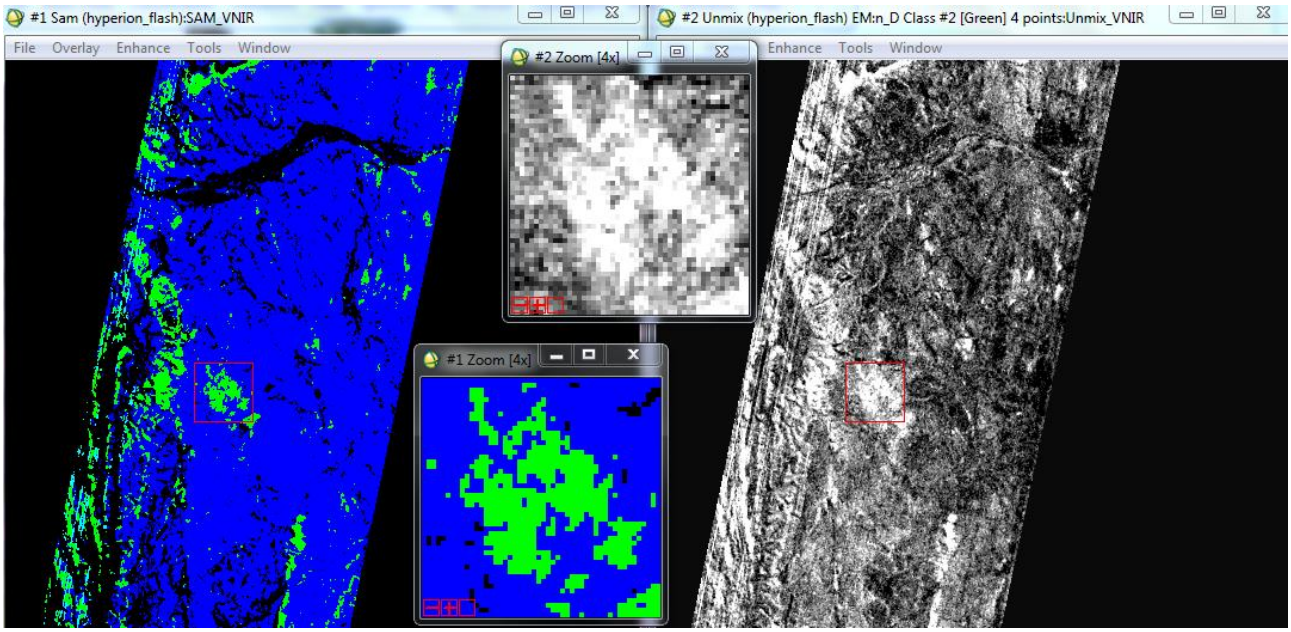

Figure 13: VNIR Spectral Unmixing Map: Alunite.
Left: SAM Classification. Right: Linear Spectral Unmixing.

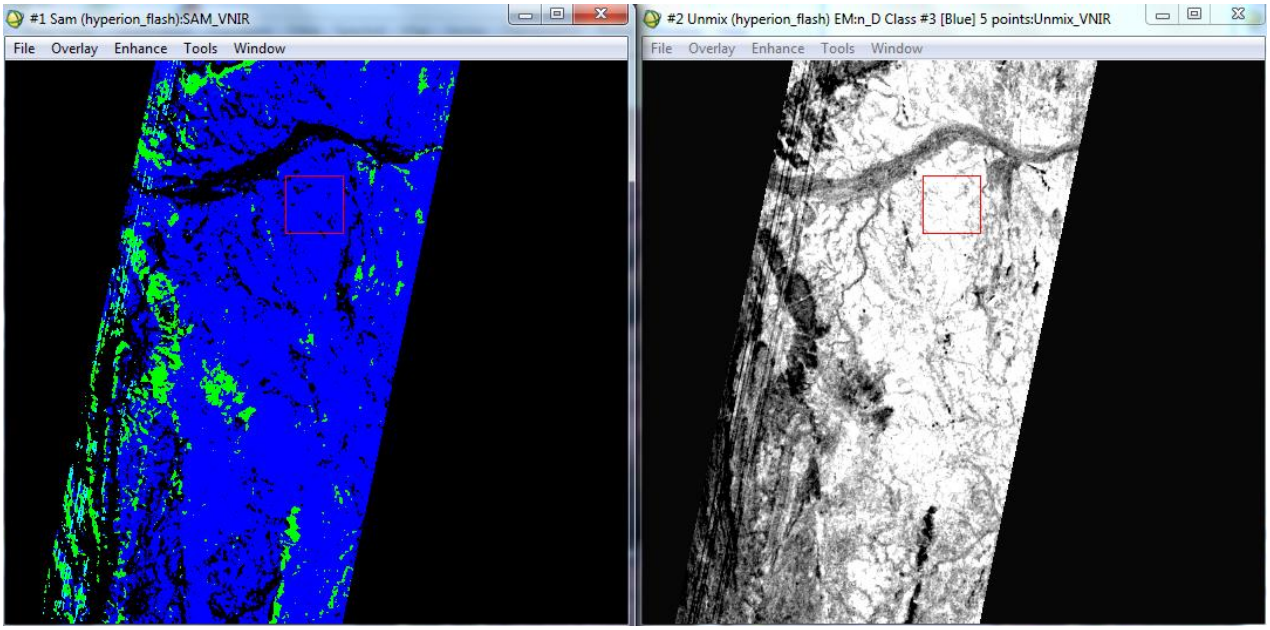

Figure 14: VNIR Spectral Unmixing Map: Hematite.
Left: SAM Classification. Right: Linear Spectral Unmixing.

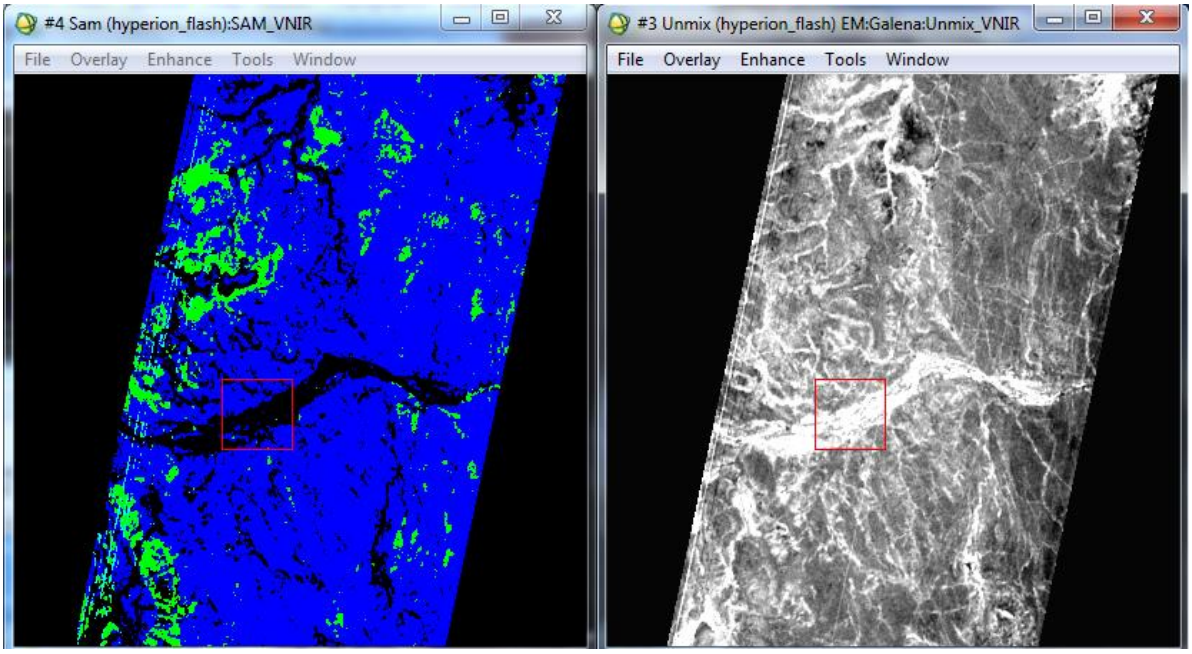

Figure 15: VNIR Spectral Unmixing Map: Galena.
Left: SAM Classification. Right: Linear Spectral Unmixing.

The hyperspectral analyses of the VNIR produced a broader classification map (SAM) and a detailed abundance map (spectral unmixing) of the study area. Compared to multispectral techniques, the SAM method seems to be a minor improvement for mineral mapping, while the spectral unmixing method was a much more effective technique.

5.2.2 SWIR Results

The analysis of the SWIR spectrum helped locate and map several sulphate and hydroxyl-bearing minerals within the study area. The spectral properties of the selected endmembers were analysed and the following minerals were found: tincalconite, gypsum, rhodonite and galena. The SAM method produced a classification map of the four minerals, but mostly mapped gypsum and galena. The yellow-coloured areas on the map represent gypsum ($CaSO_4$ $2H_2O$), a sulphate mineral, and the pink-coloured areas represent galena (PbS). This method does not compare quite as well with the multispectral analysis as did the SAM classification for the VNIR analysis (Figure 16). The areas consisting of gypsum match well with the multispectral images; however there are many more differences with the rest of the data. The SAM classification method does not seem to be the best method for the SWIR in hyperspectral images.

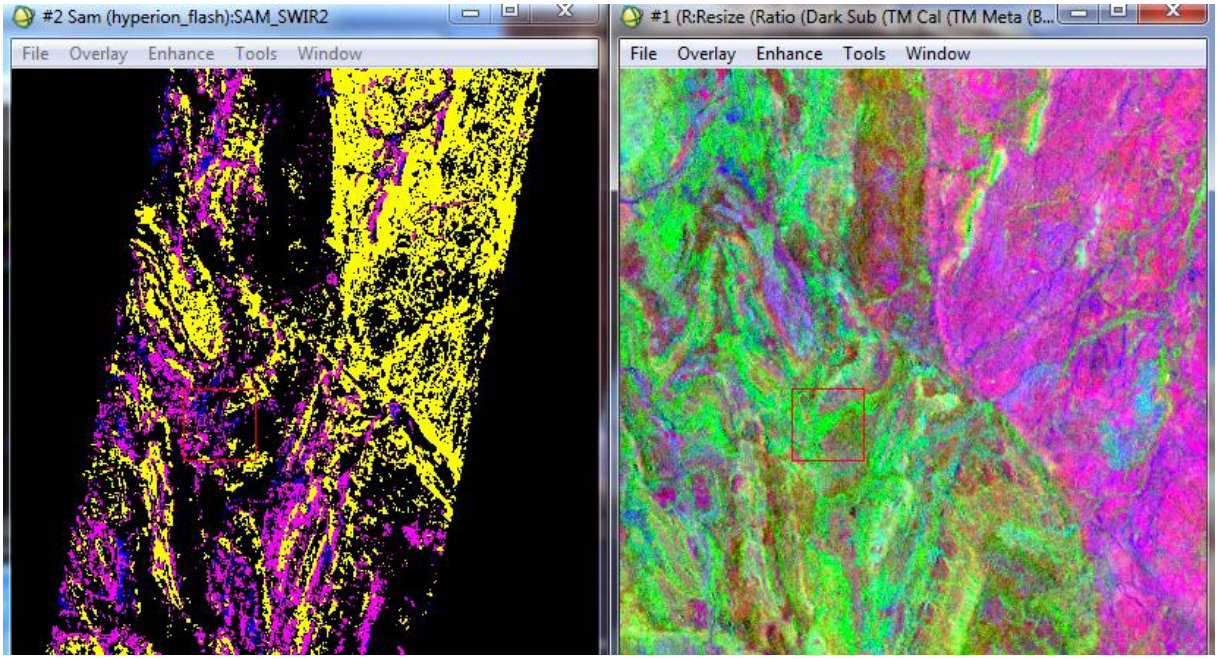

Figure 16: SWIR SAM Classification Map.
Left: SAM Classification. Right: Landsat 5 TM band ratio 3/1, 5/7, 5/4.

The linear spectral unmixing method again produced several gray-scale images of each mineral showing the bright pixels as high abundances of that mineral within the image. This method worked best with tincalconite ($Na_2[B_4O_5(OH)_4]$ $3H_2O$), a hydroxyl-bearing sodium mineral, and gypsum. The higher abundances of tincalconite are located in areas that were not mapped in the SAM method, which were left black (Figure 17). The SAM method and spectral unmixing method both have mapped gypsum in very similar areas, as seen from the yellow-coloured areas in the SAM maps (Figure 18). The spectral unmixing method also mapped a large amount of rhodonite ($FeSiO_3$), an iron-bearing silicate mineral, which has been mapped in the black and yellow-coloured areas with respect to the SAM maps (Figure 19). This mineral was barely mapped by the SAM method, most likely because it could be mixed in rocks with more abundant minerals such as gypsum.

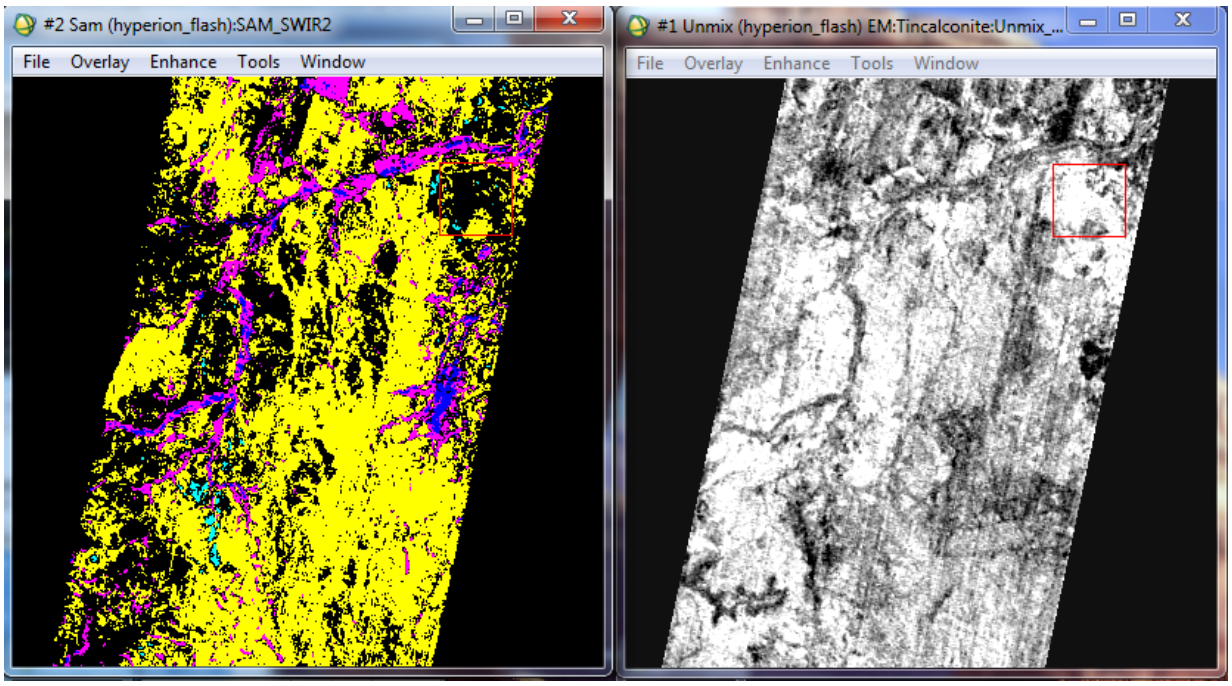

Figure 17: SWIR Spectral Unmixing Map: Tincalconite.
Left: SAM Classification. Right: Linear Spectral Unmixing.

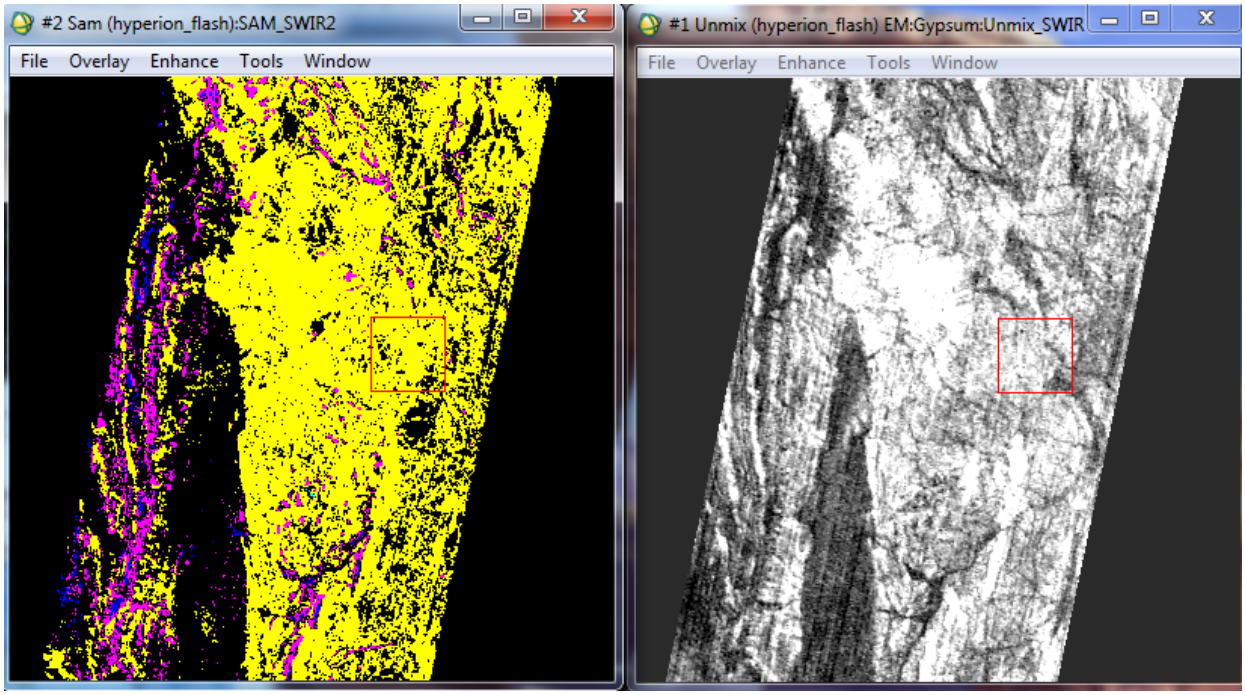

Figure 18: SWIR Spectral Unmixing Map: Gypsum.
Left: SAM Classification. Right: Linear Spectral Unmixing.

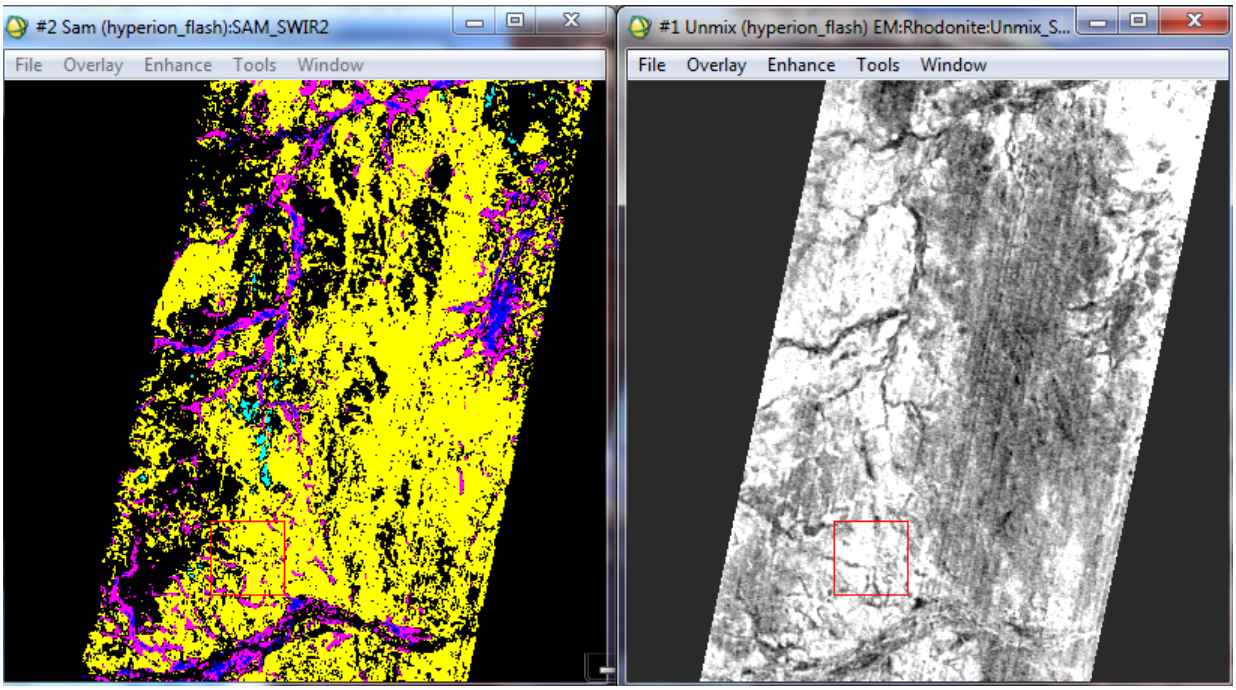

Figure 19: SWIR Spectral Unmixing Map: Rhodonite.
Left: SAM Classification. Right: Linear Spectral Unmixing.

The SWIR analysis is much harder to interpret due to the various differences between the SAM method, spectral unmixing method and the multispectral results. Hydroxyl-bearing minerals, sulphates and iron-bearing minerals were all mapped with the spectral analyses of the SWIR. These results still conclude that there are potential mining sites within the northern section of the study area.

From the results of both the VNIR and SWIR analyses, the most probable ores that could be mined are lead or iron. However, the analyses also showed many areas with hydroxyl-bearing minerals and thus

hydrothermally altered rocks which could produce different minerals at further depths. Before any subsequent steps are taken in the mineral exploration process, a field survey must be conducted in order to verify the results of these analyses.

6. Conclusion

This mineral exploration study identified several potential mining locations for iron-oxide, sulphate and hydroxyl-bearing minerals in North West Queensland, Australia. A multispectral analysis using false-colour composites and band ratio composite revealed that the northern portion of the study area was composed of rocks containing iron-oxides and sulphates generally in northeast and rocks containing hydroxyl-bearing minerals mostly in the northwest. A PCA produced a more detailed location map of these mineral types, displaying more of the hydroxyl-bearing minerals in the mid-west region of the area. A hyperspectral analysis of both the VNIR and SWIR spectrums revealed even more detail of the study area by providing location and abundance maps of specific minerals including alunite, hematite, galena, gypsum and tincalconite. This mixture of sulphate and iron- and hydroxyl-bearing minerals was mapped in detail using both SAM and spectral unmixing techniques, which produced classification and abundance maps, respectively. These methods yielded similar results to the multispectral results, showing mostly sulphates and iron-oxides in the northeast and hydroxyl-bearing minerals in the northwest.

The multispectral and hyperspectral analyses revealed that there are plenty of potential mining opportunities located in the northern section of the study area. Several different remote sensing techniques can be used to analyse different parts of the electromagnetic spectrum and provide detailed maps for mineral exploration. This study can be applied to other locations with similar environments and conditions in order to assist with mineral exploration and mining.

7. References

Amax, M. J., Brown, D, et al. (1983). “Remote sensing for porphyry copper deposits in southern Arizona.” Economic Geology **78**: 591-604.

Bishop, C. A., J. G. Liu, et al. (2011). "Hyperspectral remote sensing for mineral exploration in Pulang, Yunnan Province, China." International Journal of Remote Sensing **32**(9): 2409-2426.

Cloutis, E. A. (1996). "Hyperspectral geological remote sensing: Evaluation of analytical techniques." International Journal of Remote Sensing **17**(12): 2215-2242.

Conaghan, E. L., K. W. Hannan, J. Tolman (2003). “Mount Isa Cu and Pb-Zn-Ag deposits, NW Queensland, Australia.” CRC LEME Open-file report, Version 1.1.

Crosta, A. P., C. R. De Souza, et al. (2003). "Targeting key alteration minerals in epithermal deposits in Patagonia, Argentina, using ASTER imagery and principal component analysis." International Journal of Remote Sensing **24**(21): 4233-4240.

Dehnavi, A. G., R. Sarikhani and D. Nagaraju (2010). “Image processing and analysis of mapping alteration zones in environmental research, east of Kurdistan, Iran.” World Applied Science Journal **11**(3): 278-283.

Denniss, A., J. Huntington, et al. (1999). “Mount Fitton hyperspectral mineral mapping collaborative project.” MESA Journal (15): 12-14.

Goetz, A. F. H., G. Vane, et al. (1985). "Imaging Spectrometry for Earth Remote-Sensing." Science **228**(4704): 1147-1153.

Goetz, A. F. H. and L. C. Rowan (1981). "Geologic Remote-Sensing." Science **211**(4484): 781-791.

Harris, J. R., A. N. Rencz, et al. (1998). "Mapping altered rocks using Landsat TM and lithogeochemical data: Sulphurets-Brucejack Lake district, British Columbia, Canada." Photogrammetric Engineering and Remote Sensing **64**(4): 309-322.

Imbroane, A., M. Cornelia, et al. (2007). "Mineral explorations by Landsat image ratios." In *Ninth International Symposium on Symbolic and Numeric Algorithms for Scientific Computing*, 26-29 September. Timisoara, Romania.

McDonald, G. D., K. D. Collerson and P. D. Kinny (1997). "Late Archean and early Proterozoic crustal evolution of the Mount Isa block, northwest Queensland, Australia." Geology **25**(12): 1095-1098.

Mshiu, E. E. (2011). "Landsat remote sensing data as an alternative approach for geological mapping in Tanzania: A case study in the Rungwe Volcanic Province, south-western Tanzania." Tanzania Journal of Science **37**(1): 26-36.

Oliver, S. and S. van der Wielen (2006). "Mineral mapping with ASTER." AusGeo News **82**.

Rajesh, H. M. (2004). "Application of remote sensing and GIS in mineral resource mapping - An overview." Journal of Mineralogical and Petrological Sciences **99**(3): 83-103.

Resmini, R. G., M. E. Kappus, et al. (1997). "Mineral mapping with HYperspectral Digital Imagery Collection Experiment (HYDICE) sensor data at Cuprite, Nevada, U.S.A." International Journal of Remote Sensing **18**(7): 1553-1570.

Rockwell, B. W. (2004). "Spectral variations in rocks and soils containing ferric iron hydroxide and (or) sulphate minerals as seen by AVIRIS and laboratory spectroscopy." USGS Open-file report, Version 1.2.

Sabins, F. F. (1999). "Remote sensing for mineral exploration." Ore Geology Reviews **14**(3-4): 157-183.

Tukiainen, T. and B. Thomassen (2010). "Application of airborne hyperspectral data to mineral exploration in North-East Greenland." Geological Survey of Denmark and Greenland Bulletin(20): 71-74.

van der Meer, F. D., H. M. A. van der Werff, et al. (2012). "Multi- and hyperspectral geologic remote sensing: A review." International Journal of Applied Earth Observation and Geoinformation **14**(1): 112-128.

Wand, Z. H. and C. Y. Zheng (2010). "Rocks/minerals information extraction from EO-1 Hyperion data base on SVM." Paper preseneted at ICICTA conference, Changsha, China, 11-12th May.